*Exp. Theo. NANOTECHNOLOGY* 10 (2026) 535-549 https://doi.org/10.56053/10.2.535

# Nanodata technology of aerosol index over Iraq during 2005-2020

*Anmar Dherar Kosaj[1], Iqbal H. Abdulkareem[2], Osama T. Al-Taai[3,*], Zainab M. Abbood[3], Jasim H. Kadhum[3]*

[1]Department of Physics, College of Education for Pure Sciences, University of Anbar, Anbar, Iraq.
[2]The Scientific Affairs Department, Al-Iraqia University, Baghdad, Iraq.
[3]Department of Atmospheric Sciences, College of Science, Mustansiriyah University, Baghdad, Iraq.
[*)] Email: osamaaltaai77@uomustansiriyah.edu.iq

*Received* 13/1/2026, *Received in revised form* 16/2/2026, *Accepted* 11/3/2026, *Published* 15/4/2026

The Aerosol Index (AI) is a measure of the number of UV-absorbing aerosols in the air, such as soot and desert dust. The AI is positive for absorbing aerosols and negative for non-absorbing aerosols. AI is derived from the Ozone Monitoring Instrument (OMI) on board the Dutch–Finnish Aura satellite. In this work AI is analyzed over Iraq for the period 2005 to 2020. The results show significant spatial and temporal variabilities of the seasonal AI with lower (<1) at the southern parts and higher (>2) at the southern part. The AI is significantly changes from season to season being low during winter and high during summer. AI in spring is higher than that in autumn, especially in the south, due to more frequent northwesterly wind. The effect of rain shortage and the large NW Shamal wind on AI are apparent since AI is very high along the alluvial plain during summer The box, whisker plots of mon AI for six cities, chosen to consist of different regions of Iraq, show that Mosul records the lowest minimum AI (~0.1) and the lowest average (~1.1). Anah exhibits the highest maximum AI (~4.1), while Basra has the highest mean value (~2.0). Outliers in AI are observed only in Rutba (two cases) and Al-Nukhaib (one case). Mann-Kendall test on the seasonal AI of the six cities indicates a significant decreasing trend of AI is observed during summer season in all cities and the trend is most significant in Mosul, Anah, Baghdad, and Basra. The most decreasing trend during Autumn occurred in the city of Basra. AI contours overlaid on MODIS false colors images in three different dust storms cases and one non-dust case revels that AI can provide information on the severity, gradient, location of core, and tracking path of a dust storm.

**Keywords:** AI; OMI; Dust storms; Nanodata.

## 1. INTRODUCTION

Dust storms are common natural phenomena in arid and semi-arid regions of the world, especially within subtropical latitudes. These events are typically associated with strong winds that transport large amounts of dust particles across wide areas, producing several environmental and societal impacts [1]. One of the most noticeable consequences is the sharp decrease in horizontal visibility, which can disrupt many human activities, increase the risk of traffic accidents, and sometimes lead to the suspension of air transportation [2,3]. Dust storms can have significant environmental impacts, including the reduction of soil fertility, damage to crops, and a decrease in the amount of solar radiation reaching the surface, which may reduce the efficiency of solar energy systems. They can also affect communication and mechanical systems, increase air pollution, and contribute to respiratory health issues [4,5]. In the Middle East, these events are most common during spring and summer, particularly in countries such as Iraq, Kuwait, Saudi Arabia, and Iran [6]. Modeling studies have estimated that roughly 20% of global dust emissions originate from this region [7,8]. Within Iraq, ten main dust source areas have been identified, covering about 16% of the country, with the majority located in the Tigris and Euphrates basins [9–11]. The Aerosol Index (AI), taken from ultraviolet reflectance measurements by the Ozone Monitoring Instrument (OMI), serves as an effective indicator of absorbing aerosols in atmosphere [12,13]. AI data have been widely used to detect dust events, track their transport, and identify source regions. For instance, combining AI with brightness temperature from the Advanced Microwave Sounding Unit (AMSU) has been used to confirm dust storm events over India's Indo-Gangetic Plain [14]. Long-term AI records (1979–2011) have helped identify major global dust source regions, showing that high AI values are typically found in arid and semi-arid areas, and that dust is strongly influenced by geomorphology and regional weather patterns [15]. Other studies have demonstrated AI's usefulness in detecting surface dust conditions and its association with meningitis outbreaks in the Sahel region of Africa [16]. Additionally, AI has been applied to identify dust source regions impacting Kuwait [17] and to examine the spatial and temporal of aerosols over Pakistan, where higher AI values are observed in the south compared with the north [18]. Given its long-term availability since 1979, AI remains a key dataset for studying dust storm climatology [19]. Furthermore, AI observations have been integrated with meteorological data and true-color satellite imagery from the Moderate Resolution Imaging Spectroradiometer (MODIS) to enhance the monitoring of dust storm events [20,21]. Used SCIAMACHY AI for the period 2003-2012 to assess dust variability in Iraq. His results indicated that the dust activities depend on proximity to the dust source area and on the season of the year [22]. A previous study examined dust storms in North Africa using the Weather Research and Forecasting (WRF) model together with AI observations and dust records collected from about 300 meteorological stations over a period of two decades. The study indicated that dust emissions are mainly generated by two mechanisms: dynamically driven dust storms and thermally driven dust devils. The results also showed that dust storm activity is most frequent during the spring season and that the spatial and temporal patterns of AI are more closely related to dust devil emissions. Another study analyzed the spatial and temporal variability of aerosol optical depth (AOD) and Aerosol Index (AI) over the Indian subcontinent. The findings suggested that elevated AI values during the pre-monsoon period are associated with increased aerosol loading and the transport of ultraviolet-absorbing dust particles across the region [23]. Dust storms are common natural phenomena in arid and semi-arid regions of the world, especially within subtropical latitudes.

These events are typically associated with strong winds that transport large amounts of dust particles across wide areas, producing several environmental and societal impacts [1]. One of the most noticeable consequences is the sharp decrease in horizontal visibility, which can disrupt many human activities, increase the risk of traffic accidents, and sometimes lead to the suspension of air transportation [2,3]. Dust storms can have a range of environmental impacts, including reduced soil fertility, crop damage, and lower solar radiation reaching the surface, which may decrease the performance of solar energy

systems. These storms can also disrupt communication and mechanical equipment, contribute to air pollution, and increase respiratory health risks [4,5]. In the Middle East, dust storms are most frequent during spring and summer, particularly in Iraq, Kuwait, Saudi Arabia, and Iran [6]. Modeling studies suggest that this region accounts for approximately 20% of global dust emissions [7,8]. Within Iraq, ten major dust source areas have been identified, covering around 16% of the country, mostly concentrated in the Tigris and Euphrates River basins [9–11]. The Aerosol Index (AI), derived from ultraviolet reflectance measurements from the Ozone Monitoring Instrument (OMI), is widely used to detect and monitor absorbing aerosols in the atmosphere [12,13]. AI has been applied to track dust events, determine their transport, and identify source regions. For instance, combining AI with brightness temperature from the Advanced Microwave Sounding Unit (AMSU) has been used to confirm dust storms over India's Indo-Gangetic Plain [14]. Analyses of AI records from 1979 to 2011 have also identified major global dust source areas, showing that high AI values occur mainly in arid and semi-arid regions, and that dust distribution is influenced by geomorphology and regional meteorology [15]. Furthermore, AI has proven useful in identifying surface dust conditions and exploring links with meningitis outbreaks in the Sahel region of Africa [16]. It has also been used to identify dust sources affecting Kuwait [17] and to study the spatial and temporal of aerosols over Pakistan, where higher AI values are generally observed in the south regions compared with the north [18]. Because AI data have been available since 1979, they provide a valuable resource for investigating the climatology of DS[19]. Furthermore, AI observations have been integrated with meteorological data and true-color satellite imagery from the Moderate Resolution Imaging Spectroradiometer (MODIS) to enhance the monitoring of dust storm events [20,21]. The objective of this study is to examine the Aerosol Index (AI) obtained from OMI observations over Iraq during the period 2005–2020 and to investigate the variations of this index in relation to dust storm activity [24,25].

## 2. MATERIALS AND METHODOLOGY

### *2.1 Area of study*

Iraq is located in the Middle East and covers an area of about 437,072 km², with a population exceeding 38 million people. The geographical location and major topographic divisions of Iraq are illustrated in Figure 1 [26]. The country is bordered by Turkey to the north, Iran to the east, Kuwait to the south, the Kingdom of Saudi Arabia (KSA) to the south and southwest, and both Jordan and Syria to the west [27]. From a topographical perspective, Iraq is commonly classified into four main regions. The mountainous region occupies the northern and northeastern parts, while the alluvial plain extends across the central and southeastern areas. In addition, upland areas stretch from the northwest toward the southwest, and the western part of the country is dominated by a high desert landscape [28]. Climatically, most parts of Iraq experience arid to semi-arid conditions, characterized by very hot and dry summers and relatively mild to cold winters [29]. Precipitation is mainly concentrated between October and May, with an annual mean rainfall of around 200 mm [30]. Dust storms represent a frequent meteorological phenomenon in Iraq and may occur throughout the year, although they are more common during spring and summer.

These events are often associated with the Shamal wind, which can persist for several days and transport large quantities of dust toward the Arabian Gulf and neighboring as Kuwait, Saudi Arabia, and Iran [31]. Earlier research has highlighted ten primary dust source areas in Iraq, together covering about 16% of the country's total land [10]. Among them, two regions are particularly active. One is located in the northeast, considered an extension of dust sources from Syria, while the other lies near the southern border adjacent to Saudi Arabia and Kuwait.

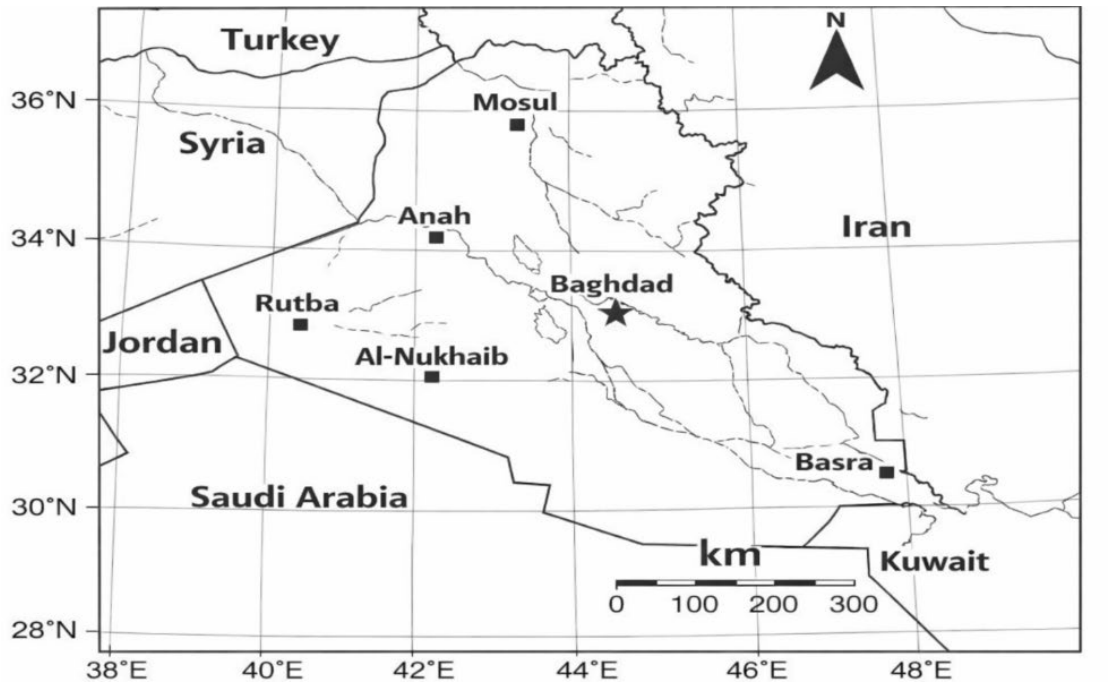


**Figure 1** Study stations in Iraq map.

*2.2 Data sources*

To carry out this study, several datasets are utilized, including Aerosol Index (AI) data derived from the Ozone Monitoring Instrument (OMI). The OMI sensor is mounted on board the AURA satellite, which is launched in Jul 2004 together with 3 additional instruments [32]. This instrument measures backscattered radiation that is used to retrieve different atmospheric aerosol properties, including the Aerosol Index (AI) [18]. The concept of AI is originally introduced by Torres using radiance measurements from the Total Ozone Mapping Spectrometer (TOMS) at wavelengths of 340 and 380 nm. Later, the formulation is adapted for OMI observations using wavelengths of 354 and 388 nm [33,34].

$$A = -100 \log_{10}\left(\frac{I_{abs.}^{354}}{I_{calc.}^{354}}\right) \quad (1)$$

Here, $(I_{abs.}^{354})$ represents the radiance measured by the satellite at 354 nm, while $(I_{calc.}^{354})$ is the radiance estimated from AI at 388 nm. Positive AI values indicate the presence of absorbing aerosols, such as dust and smoke, whereas negative values correspond to non-absorbing aerosols. To examine the potential influence of precipitation on the space and time patterns of dust activity, monthly accumulated rainfall data are obtained from the Tropical Rainfall Measuring Mission (TRMM) throughout the study period. TRMM is a collaborative satellite mission developed by the United States National Aeronautics and Space Administration (NASA) and the Japan Aerospace Exploration Agency (JAXA). For this study, monthly gridded Aerosol Index (AI) data with a space resolution of 1° × 1°, covering Iraq (38.5–49.5°E longitude and 28.5–37.5°N latitude) for 2005–2018, are obtained from the Tropospheric Emission Monitoring Internet Service (TEMIS).

Additionally, monthly accumulated precipitation data with a finer spatial resolution of 0.25° × 0.25° are retrieved from the Giovanni data portal. To analyze specific dust storm events, daily MODIS false-color imagery is downloaded from the NASA Worldview platform. The prevailing wind characteristics over Iraq are investigated using long-term wind rose analysis based on the monthly zonal and meridional

wind components. These meteorological data are obtained from the European Centre for Medium-Range Weather Forecasts (ECMWF). Finally, the Mann–Kendall statistical test is applied to evaluate the long-term trends in the dataset [17,35].

### *2.3 Nano data technology*

Nano data technology refers to the integration of nanoscale sensors, devices, and systems for acquiring, processing, and analyzing environmental, physical, or biological data. With advancements in nanotechnology, sensors at the nanometer scale can detect phenomena with unprecedented sensitivity, including air quality parameters, temperature, pressure, and chemical composition. Applications of nano data technology include [36-41]:

1. Air pollution monitoring ($PM_{2.5}$, $PM_{10}$, NOx, SOx, $O_3$).
2. Climate and meteorological research.
3. Precision agriculture (soil moisture, nutrient detection).
4. Health and biomedical diagnostics.

## 3. RESULTS AND DISCUSSION

The upper part of Figure 2 illustrates the seasonal spatial pattern of the Aerosol Index (AI) across Iraq. It can be observed that the northern mountainous regions, the northeastern areas, and the western desert generally exhibit the lowest AI values (less than 1) throughout all seasons. In contrast, the southern parts of the country show relatively higher values, often exceeding 2.0. The results further suggest that dust activity in Iraq typically begins to increase during the spring season, reaches its maximum during the summer months, and then gradually declines during autumn. The lowest levels of dust activity are generally recorded in the winter season. The spatial distribution also illustrates that AI is increasing from northwest (near the borders with Syria) to southwest border regions with KSA and Kuwait. This behavior of AI over Iraq can be attributed to the prevailing wind and precipitation. As seen in the middle and lower panels of Figure 2, rain falls mostly on the north and northeastern mountain areas. In Iraq, rain activities begin in October and last until May but most rain storms occur during winter months. Also, during these months wind is weak and may blow from any direction. Presence of rain and weak wind during autumn and winter reduce dust activities during these two seasons. This explains the relatively low values of AI during autumn and winter. In spring the north westerly Shamal wind starts to prevail and becomes stronger during summer months [42-46].

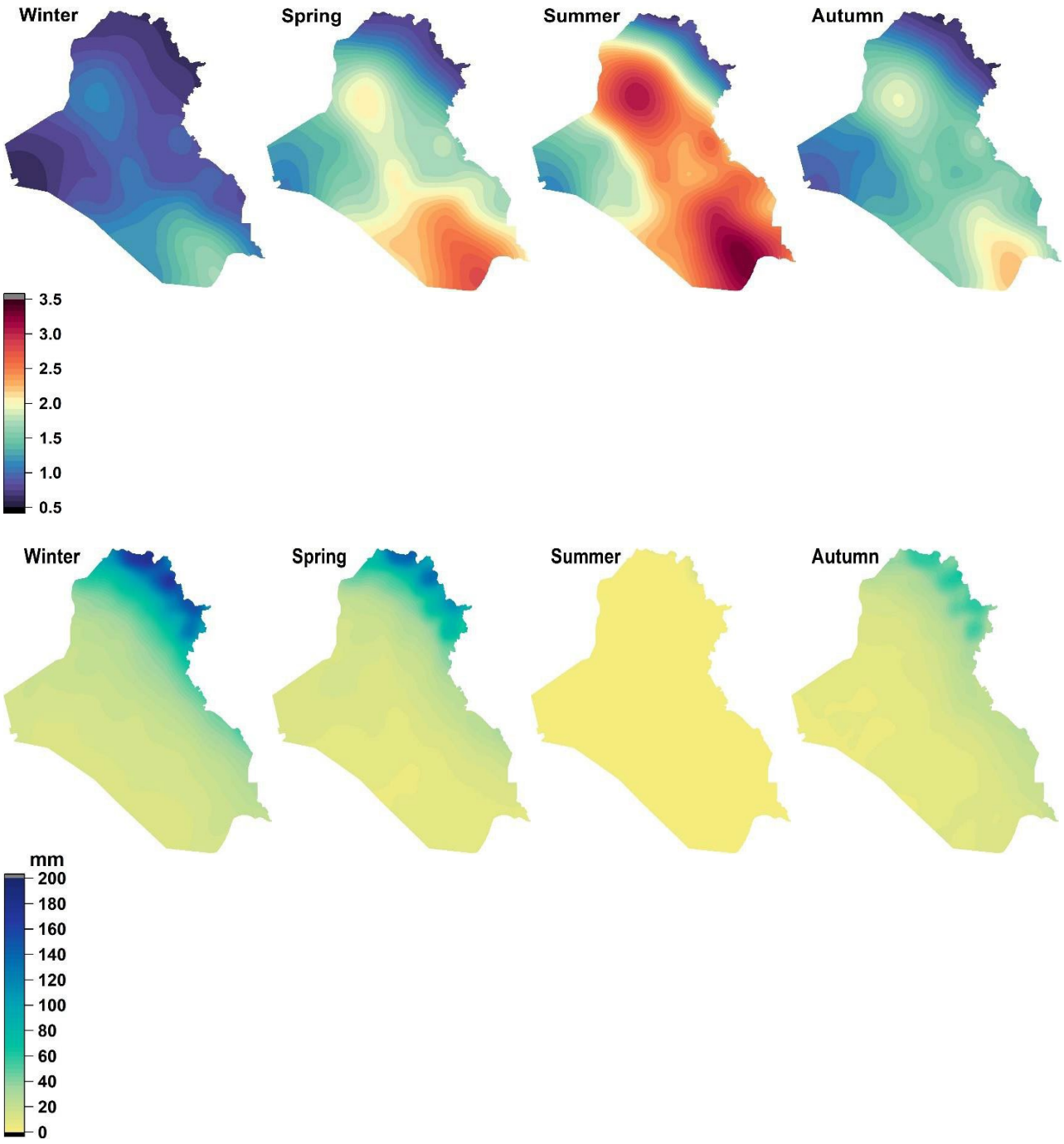
Winter
Spring
Summer
Autumn
3.5
3.0
2.5
2.0
1.5
1.0
0.5
Winter
Spring
Summer
Autumn
mm
200
180
160
140
120
100
80
60
40
20
0

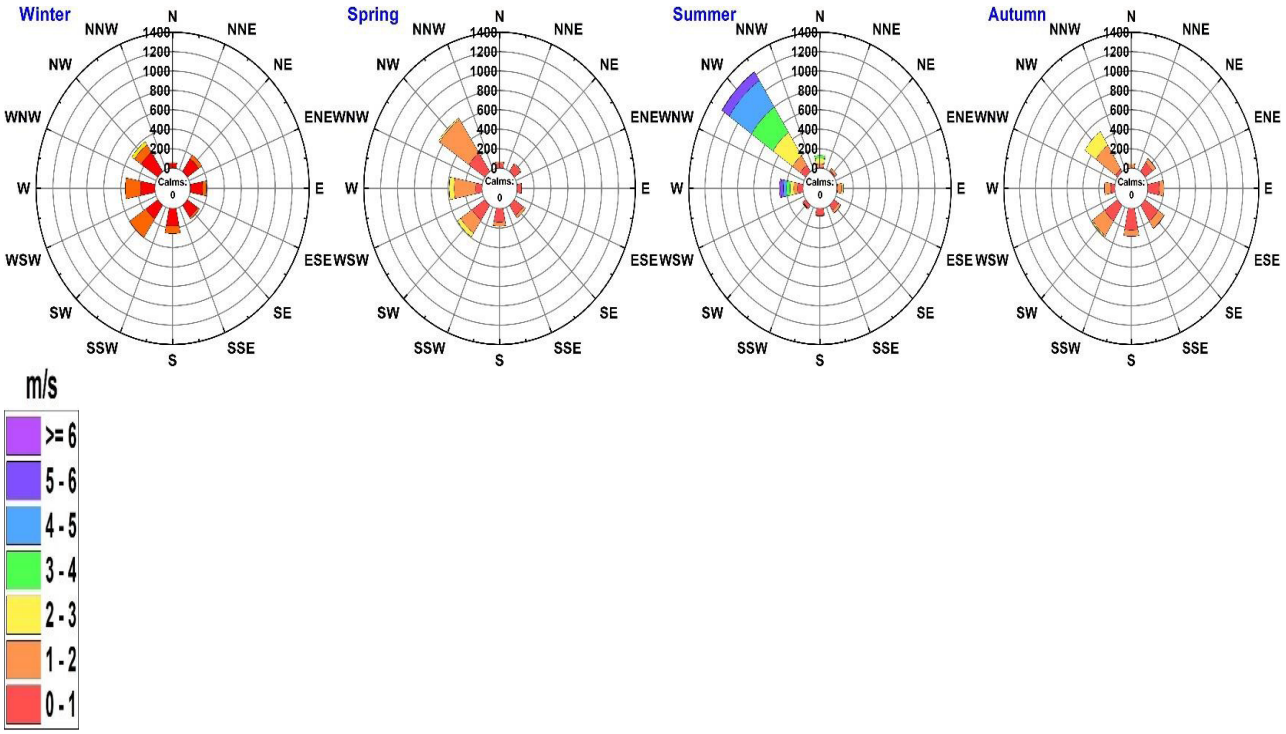


**Figure 2** Long-term seasonal AI (upper panel), seasonal rainfall (middle panel), and seasonal wind rose during 2005-2020.

The findings suggest that wind speeds can exceed 5 m/s during the summer months, which may explain the relatively high AI values observed in this season. The two prominent high-AI regions located in the northwest and southwest correspond to the main dust source areas in Iraq. The spatial pattern of AI also indicates that the southern regions generally record higher values compared with other parts of the country. This pattern can be attributed not only to the active dust sources near the Kuwaiti border but also to the influence of the Shamal wind, which transports dust from the Syrian desert and the alluvial plain. Figure 3 presents the monthly temporal variation of AI for six selected cities is different topographic and climatic zones across Iraq. The pattern of the distribution is quite equals the seasonal distribution discussed above, that is AI is low winter and high summer in all cities. The results also show that the north city of Mosul and western desert town of Rutba are characterized by the lowest values of AI while high AI values are seen in the central city of Baghdad and the western city of Anah. The high values of AI are attributed to their proximity to the major north western source of dust. AI is moderate in the western desert town of Al- Nukhaib. The most southern city of Basra is characterized by the highest AI among the six cities due the dust from the nearby most effective source of dust particles and dust carried the Shamal wind from sources along the alluvial plain. The results also show that AI varies from year to year. The reason for these variations is mainly attributed to the variations of rain from one season to another. In Iraq, dry rain season is usually followed by more dust activities in spring and summer and vis versa. Comparing AI pattern with the annual rainfall for the six cities (Figure 4) shows that AI is notably high when rainfall is low (e.g. 2008 and 2009). The results clearly show how the unusual heavy rain storms that occurred over Iraq during the last three years (2018-2020) reduced the values of AI. Box and Whisker plot is used to statistically compare the monthly values of AI for the six locations. In this plot (Figure 5) the first and third quartiles of data are drawn as a box with a horizontal line goes through the box at the median. The Whisker lines go from first and third quartiles to the minimum and maximum.

The results show that the median and mean values of AI are nearly identical for most cities, indicating a relatively balanced distribution of the data. However, in Basra the median lies below the mean, suggesting that more than half of the AI values are lower than the average. The box plots also reveal that Mosul and Rutba have similar distributions with the smallest interquartile range (IQR), which represents the interval between the first and 3 quartiles. In contrast, Anah and Basra exhibit the largest IQR values. Among the six cities analyzed, Mosul records the lowest minimum AI value (approximately 0.1) and also the lowest average value (around 1.1). On the other hand, Anah shows the highest maximum AI value (about 4.1), while Basra has the highest mean AI value (approximately 2.0). Outliers beyond 1.5 times the IQR are observed only in Rutba (two cases) and Al-Nukhaib (one case). Figure 6 presents the seasonal time series of AI for the selected cities. The seasonal variation in Mosul, Rutba, and Al-Nukhaib follows a similar pattern, with AI values generally ranging between 0.5 and 2.0. In Baghdad, seasonal AI varies from around 0.5 in winter to slightly above 2.0 during summer. For Anah and Basra, AI values remain close to 1.0 in winter but increase to more than 2.5 in the summer season. The Mann-Kendall test is employed to determine the significance of the apparent seasonal decreasing trend of AI in the six selected cities. The results, summarized in Table 1, indicate that no trend is observed during winter and a significant decreasing trend of AI is observed during summer season in all cities and the trend is most significant in Mosul, Anah, Baghdad, and Basra. The most decreasing trend during Autumn occurred in the city of Basra. As state earlier these negative trends are caused by the extreme rain events that occurred over Iraq during the past decade. The role of the Torrential rain events that dropped over Iraq during 2018 and 2019 in sharply reducing AI during summer in all locations (see Figure 4).

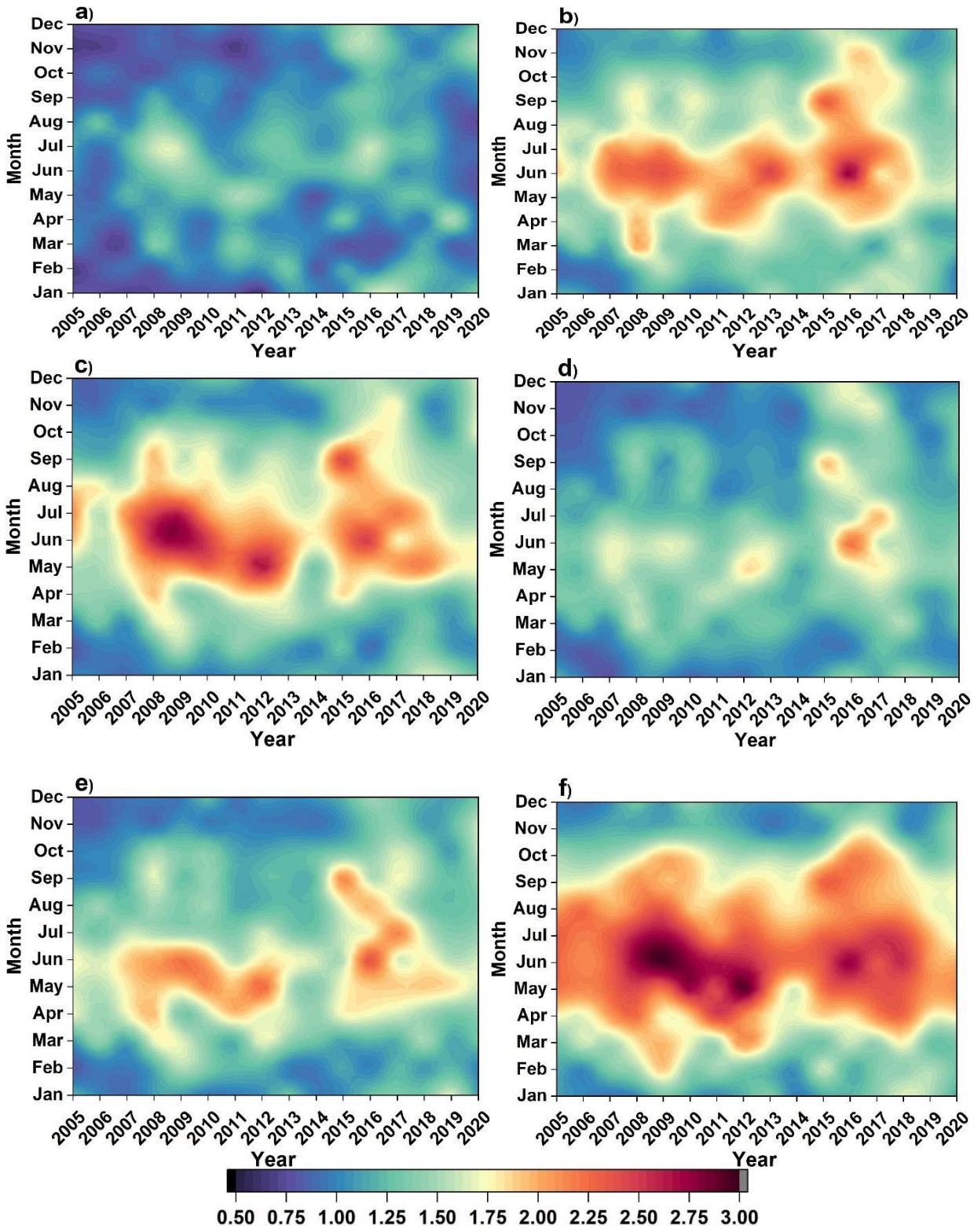


**Figure 3** Monthly variations of AI for a) Mos, b) Ana, c) Bag, d) Rut, e) Al-Nuk, and f) Bas during 2005-2020.

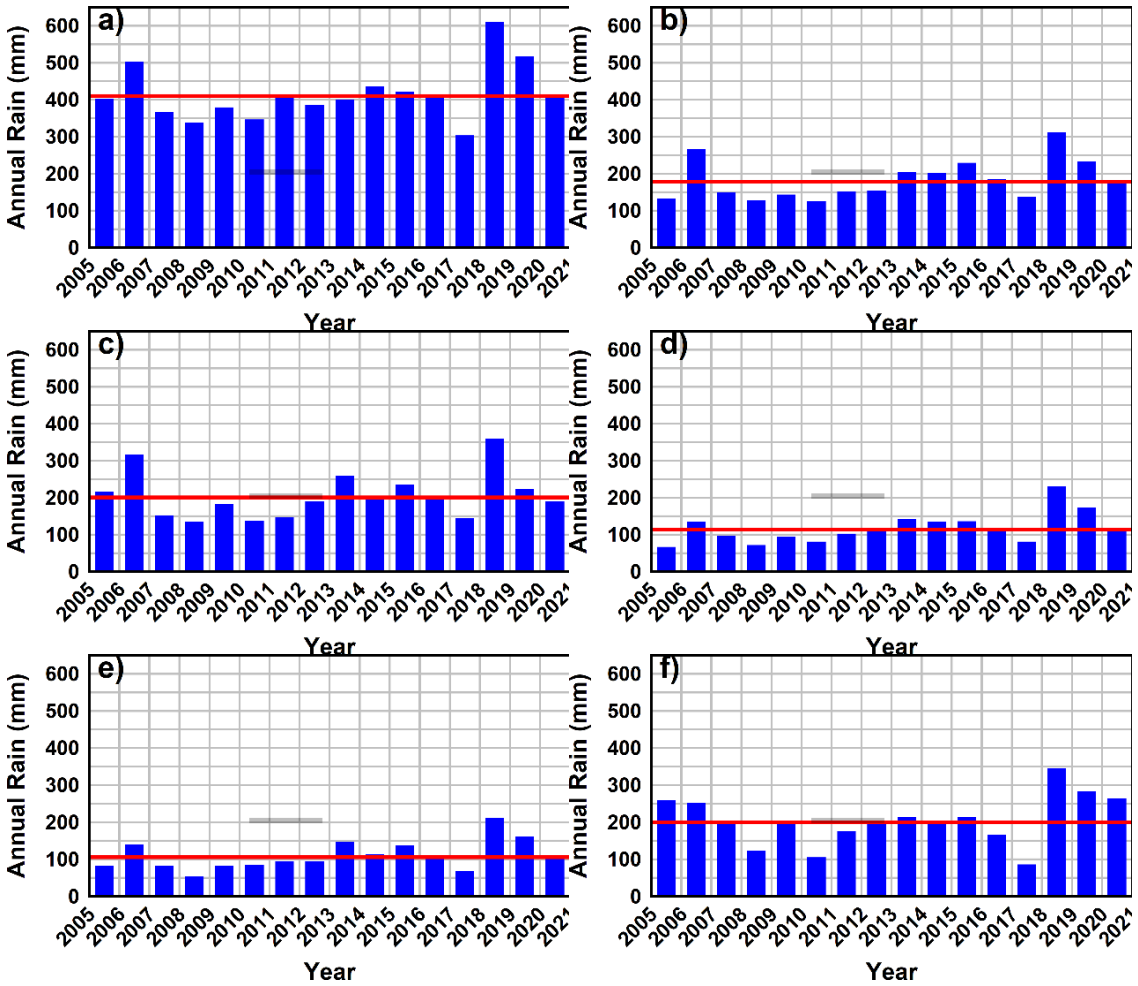


**Figure 4** Annual rainfall index for a) Mos, b) Ana, c) Bag, d) Al-Nuk, and d) Bas during 2005-2020.

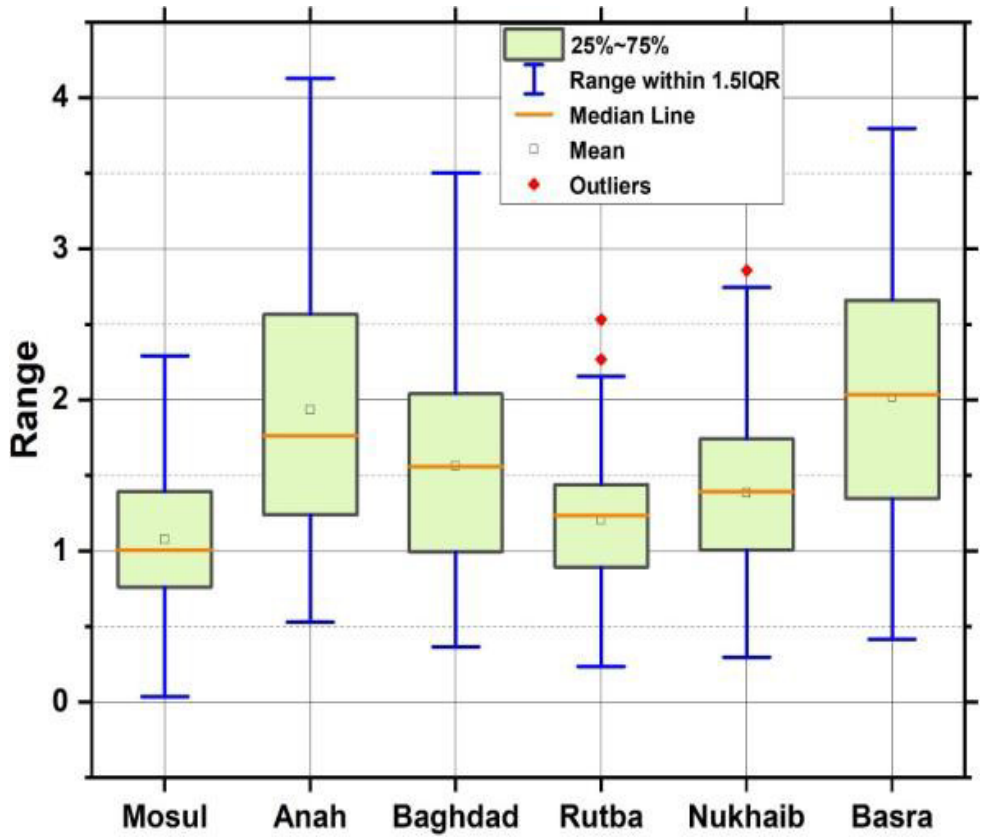


**Figure 5** Box plots of aerosols index for Mosul, Anah, Baghdad, Al- Nukhaib, and Basra during 2005-2020.

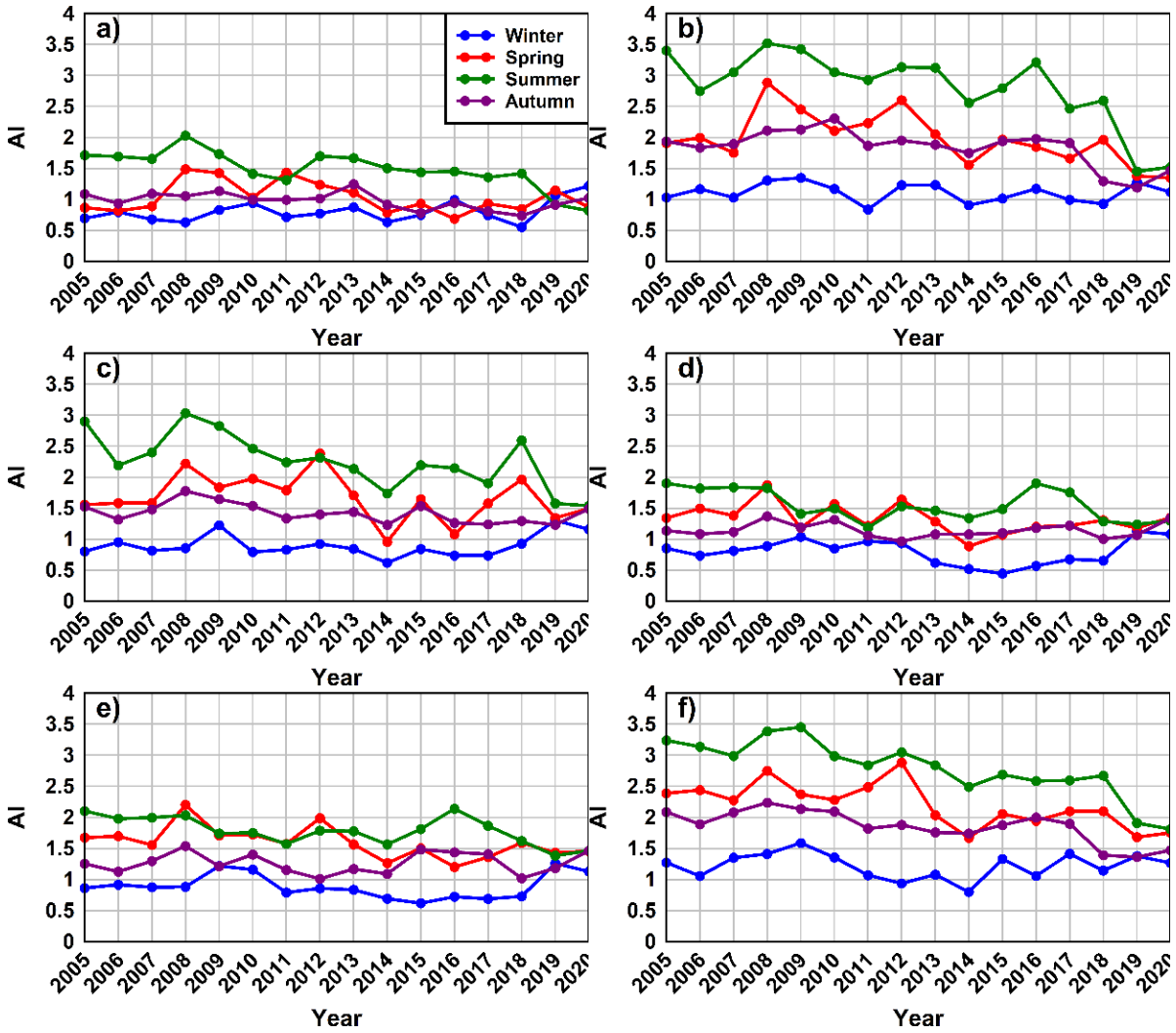


**Figure 6** Variations of seasonal aerosols index for a) Mos, b) Ana, c) Bag, d) Al- Nuk, and d) Bas during 2005-2020.

To investigate the behavior of AI during dust storms AI data are compare with MODIS false color images for four cases; three different dust cases and no dust case. Figure 7 shows AI overlaid on the MODIS images for the four cases. The false color images are composed by using a combination of infrared and visible light, dust appears beige; bare ground is brown; deep water is dark blue; vegetation is bright green; water saturated soil is light blue; snow is turquoise, and the clouds are white. A severe dust storm started from the northwestern region and moved through Iraq in the first week of July 2009. The left upper image of Figure 7 is captured on 5th of July 2009 and it is seen that the dust is so thick and obscured the ground features. The AI contours indicate that there is a high gradient from the outers of the storm towards its core where AI reached a very high value (~ 5.5). The core of the storm covered a wide area over eastern part of Iraq. The next image of Figure 7 (upper right) is captured during unusual dust storm that occurred over Iraq on 1 Sep 2015. This storm is also initiated from the same dust source area on the northwest of Iraq. The high gradients contour of AI took a cyclonic shape around the center of the storm where AI reached more than 5. Both July and September storms are spurred by the Shamal northwesterly winds. On 29 October 2017 a large dust storm covered much Iraq and northern KSA and the dust had been aloft for several days. This storm is triggered by the southeasterly Sharki winds blow toward the northwest and typically occur between November December and April. The MODIS image for this storm (lower left of Figure 7) illustrates the extends of this storm from southeast to the northwest.

The AI contours show less gradients than those in the Shamal cases and also with a lower value (~3.5) of maximum AI. The last case represents a typical clear day with no dust activities and less aerosols. The image of 29 Jan 2018 is captured after an extreme heavy rain which lasted for 48 hours. It is seen that all ground features such as lakes, marshes, and saturated soil are clearly apparent and AI ranged between 0.75 and 1.5.

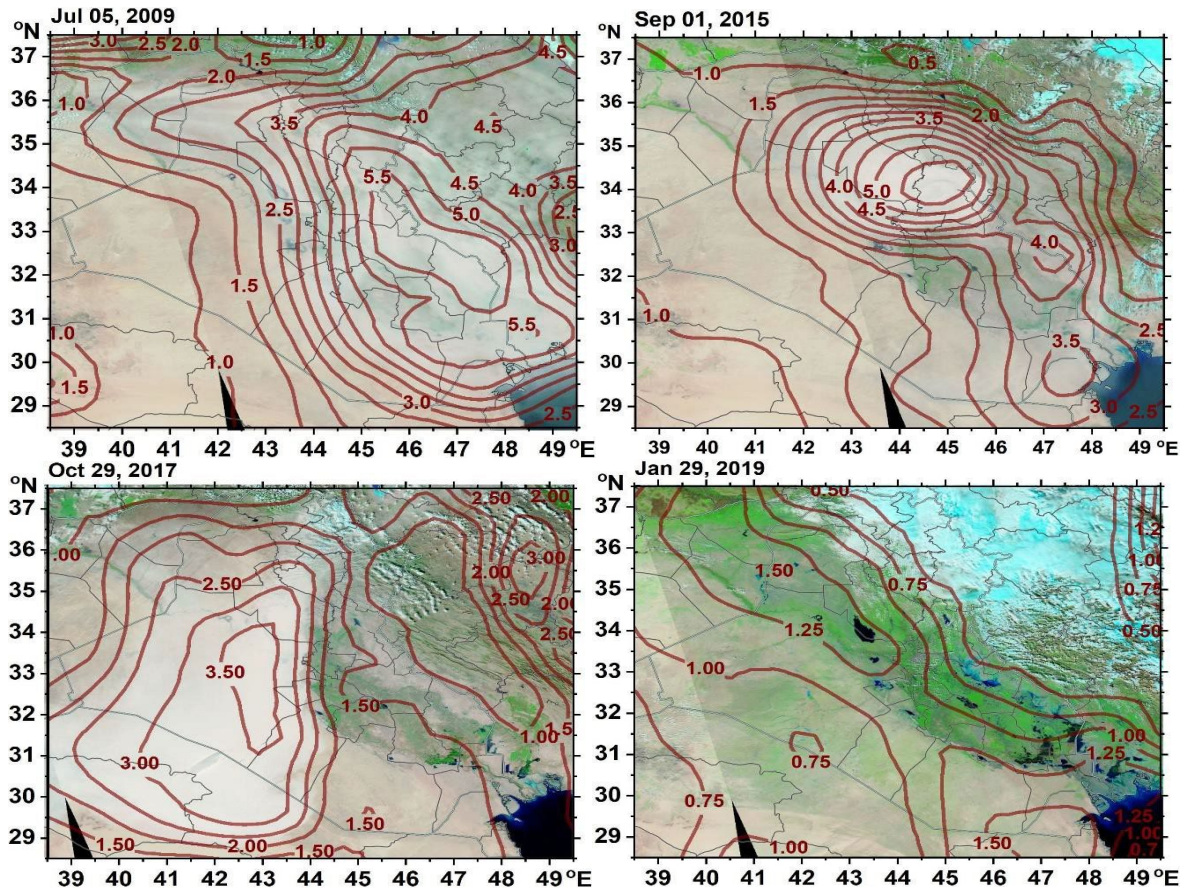


**Figure 7** Overlay of AI contours on false color images of selected dust storms over Iraq.

## 4. CONCLUSIONS

This study aimed to examine the behavior of the OMI-derived Aerosol Index (AI) over Iraq during the period 2005–2020. The seasonal spatial and temporal analysis shows that AI values are generally lowest in winter and reach their maximum during summer. During winter, dust concentrations tend to decrease as a result of rainfall and relatively weak winds. In contrast, the summer season is characterized by stronger northwesterly Shamal winds that enhance dust lifting and transport. The mountainous regions in northern Iraq consistently exhibit low AI values (less than 1) throughout the year, whereas the southern parts of the country frequently record higher values exceeding 2.0. Two main areas with particularly high AI values were identified in the northwestern and southeastern regions, indicating the presence of major dust source areas. The Shamal wind typically begins to develop during spring and intensifies during summer. This wind system lifts dust particles from the Syrian desert and from source regions located along the alluvial plain between the Tigris and Euphrates rivers, transporting them toward the southern and southeastern parts of Iraq. Consequently, the southern region generally experiences higher AI values compared with other areas due to the additional influx of transported dust. The analysis of mon AI variations for 6 selected cities representing different geographical regions in Iraq shows

noticeable differences among locations. These variations are largely influenced by the proximity of each city to major dust regions as well as the amount of precipitation received. AI also exhibited variations from year to another due to the variability of annual rainfall. Mann- Kendall test on AI seasonal time series indicated that no trend was observed during winter and a significant decreasing trend of AI was observed during summer season in all cities and the trend was most significant in Mosul, Anah, Baghdad, and Basra. Overlaying AI data on MODIS false color images for different cases of DS suggests AI may help determining the severity, gradient and core location of a dust storm and can be used to track its path.

## ACKNOWLEDGEMENTS

The authors would like to express their sincere appreciation to Mustansiriyah University, the University of Anbar, and Al-Iraqia University for their support of this research. The authors also acknowledge the use of Aura-OMI Aerosol Index (AI) data provided through the TEMIS database and the ERA-Interim reanalysis data from the European Centre for Medium-Range Weather Forecasts (ECMWF). In addition, the authors thank NASA for making MODIS imagery and TRMM precipitation data available through the Giovanni online visualization and analysis system.

## References

[1] M.A. Yehia, O.T. Al-Taai, M.K. Ibrahim, Egyptian Journal of Chemistry. 65 (2022) 1373 https://doi.org/10.21608/ejchem.2022.151633.6571
[2] R.S. Al-Awadi, O.T. Al-Taai, S.A. Abdullah, Iraqi Journal of Science, 64 (2023) 4278 https://doi.org/10.24996/ijs.2023.64.8.44
[3] W.G. Nassif, S.H. Jaber, S.S. Naif, O.T. Al-Taai, IOP Conf. Ser. Earth Environ. Sci. 910 (2021) 012010 https://doi.org/10.1088/1755-1315/910/1/012010
[4] O.T. Al-Taai, W.G. Nassif, IOP Conf. Ser. Materials Science and Engineering, 928 (2020) 072053 https://doi.org/10.1088/1757-899X/928/7/072053
[5] O.T. Al-Taai, Z.M. Abbood, Scientific Review Engineering and Environmental Sciences. 29 (2020) 196 https://doi.org/10.22630/PNIKS.2020.29.2.17
[6] O.T. Al-Taai, S.A. Hashim, W.G. Nassif, Z.M. Abbood, Journal of Physics Conference Series. 211 (2021) 012070 https://doi.org/10.1088/1742-6596/2114/1/012070
[7] M. Hamidi, M.R. Kavianpour, Y. Shao, Asia-Pacific Journal of Atmospheric Sciences. 49 (2013) 279 https://doi.org/10.1007/s13143-013-0015-8
[8] O.T. Al-Taai, W.G. Nassif, IOP Conference Series: Materials Science and Engineering. 928 (2020) 072053 https://doi.org/10.1088/1757-899X/928/7/072053
[9] W. G. Nassif, O.T. Al-Taai, Z.M. Abbood, IOP Conference Series: Materials Science and Engineering. 928 (2020) 072089 https://doi.org/10.1088/1757-899X/928/7/072089
[10] H. Cao, F. Amiraslani, J. Liu, N. Zhou, Science of the Total Environment. 502 (2015) 224 https://doi.org/10.1016/j.scitotenv.2014.09.025
[11] W.G. Nassif, I.K. Al-Ataby, O.T. Al-Taai, Z.M. Abbood, Asian Journal of Water Environment and Pollution. 21 (2024) 25 https://doi.org/10.3233/AJW240005
[12] R.S. Al-Awadi, O.T. Al-Taai, S.A. Abdullah, Experimental and Theoretical Nanotechnology. 10 (2026) 123 https://doi.org/10.56053/10.1.123
[13] A.M. Hamed, A. Razaq, A.Y. Awad, A.M. Khalaf, O.T. Al-Taai, Experimental and Theoretical Nanotechnology. 10 (2026) 141 https://doi.org/10.56053/10.1.141
[14] H. El-Askary, R. Gautam, R.P. Singh, M. Kafatos, Advances in Space Research. 37 (2006) 33 https://doi.org/10.1016/j.asr.2005.03.134
[15] G. Varga, Hungarian Geographical Bulletin. 61 (2012) 275 https://doi.org/10.15201/hungeobull.61.4.3
[16] A. Deroubaix, N. Martiny, I. Chiapello, B. Marticorena, Remote Sensing of Environment. 133 (2013) 116 https://doi.org/10.1016/j.rse.2013.02.009

[17] S.M. Robaa, Z. Al-Barazanji. Weather, 119 (2015) 493 https://doi.org/10.28974/idojaras.2015.4.6
[18] S.A. Tariq, Atmospheric Pollution Research. 6 (2014) 254 https://doi.org/10.5094/APR.2015.030
[19] S.O. Nabavi, L. Haimberger, C. Samimi, Aeolian Research. 21 (2016) 93 https://doi.org/10.1016/j.aeolia.2016.04.002
[20] K. Sun, Q. Su, Y. Ming, Remote Sensing. 11 (2019) 1772 https://doi.org/10.3390/rs11151772
[21] D. Bilal, Journal of Education for Pure Science. 9 (2019) 134 https://doi.org/10.1088/1755-1315/1215/1/012018
[22] L. Pan, Y. Han, Z. Lu, J. Li, F. Gao, Z. Liu, W. Liu, Y. Liu, Science of the Total Environment. 756 (2003) 144128 https://doi.org/10.1016/j.scitotenv.2020.144128
[23] A. Kumar. Urban Climate. 32 (2020) 1 https://doi.org/10.1016/j.uclim.2020.100598
[24] S.J. Al-Jaf, O.T. Al-Taai, Plant Archives. 19 (2019) 1450 https://doi.org/10.1088/1755-1315/1215/1/012018
[25] O.T. Al-Taai, S.A. Hashim, W.G. Nassif, Z.M. Abbood, Journal of Physics: Conference Series. 2114 (2021) 012070 https://doi.org/10.1088/1742-6596/2114/1/012070
[26] W.G. Nassif, S.H. Jaber, S.S. Naif, O.T. Al-Taai, IOP Conference Series: Earth and Environmental Science. 910 (2021) 012010 https://doi.org/10.1088/1755-1315/910/1/012010
[27] S.H. Halos, O.T. Al-Taai, M.H. Al-Jiboori, Arabian Journal of Geosciences. 10 (2017) 263 https://doi.org/10.1007/s12517-017-3058-2
[28] O.T. Al-Taai, Z.M. Abbood, J.H. Kadhum, Journal of Green Engineering. 11 (2021) 779 https://doi.org/10.28974/idojaras.2015.4.6
[29] S.A. Hashim, J.H. Kadhum, Z.M. Abbood, O.T. Al-Taai, W.G. Nassif. Nature Environment and Pollution Technology. 22 (2023) 1447 https://doi.org/10.46488/NEPT.2023.v22i03.030
[30] R. Shubbar, H. Salman, l. Dong-In, International Journal of Climatology. 37 (2016) 39 https://doi.org/10.1002/joc.4749
[31] D. Francis, C. Flamant, J.P. Chaboureau, Aeolian Research. 24 (2017) 15 https://doi.org/10.1016/j.aeolia.2016.11.001
[32] M. Schoeberl, A. Douglass, J. Joiner, Journal Geophysics Research. 113 (2008) 15 https://doi.org/10.1029/2007JD009602
[33] O. Torres, P.K. Bhartia, J.R. Herman, Journal of Geophysical Research: Atmospheres. 103 (1998) 17099 https://doi.org/10.1029/98JD00900
[34] O. Torres, A. Tanskanen, B. Veihelmann, Journal of Geophysical Research: Atmospheres. 112 (2007) 14 https://doi.org/10.1029/2007JD008809
[35] S.A. Hashim, W.G. Nassif, B.I. Wahab, Z.M. Abbood, O.T. Al-Taai, Z.S. Mahdi. Journal of Engineering Science and Technology. 17 (2022) 12 https://doi.org/10.46488/NEPT.2023.v22i03.030
[36] A.S. Hassan, J.H. Kadhum, S.N. Flashy, O.T. Al-Taai, Exp. Theor. Nanotechnology. (2025) 335 https://doi.org/10.56053/9.S.335
[37] H. K. Aity, M. Rasheed, E. Dhahri, A. A. Hateef, T. Saidani, Journal of Materials Science, 61 (2026) 6226 https://doi.org/10.1007/s10853-026-12241-w
[38] T. Saidani, S. Mokhtari, M. Rasheed, H. Lahmar, M. Trari, Journal of the Indian Chemical Society, 103 (2026) 102499 https://doi.org/10.1016/j.jics.2026.102499
[39] M. RASHEED, A. Khaleefah, Materials Chemistry and Physics, 353 (2026) 132112 https://doi.org/10.1016/j.matchemphys.2026.132112
[40] S. S. Batros, M. Rasheed, H. K. Aity, A. A. Hatef, T. Saidani, Materials Chemistry and Physics, 355 (2026) 132243 https://doi.org/10.1016/j.matchemphys.2026.132243
[41] A. Raghdi, M. Heraiz, M. Rasheed, A. Keziz, Journal of the Indian Chemical Society, 101 (2024) 101413 https://doi.org/10.1016/j.jics.2024.101413
[42] Z. S. Ahmed, M. RASHEED, H. S. Ahmed, Experimental and Theoretical NANOTECHNOLOGY 10 (2026) 329 https://doi.org/10.56053/10.s.329
[43] Z. S. Ahmed, M. RASHEED, H. S. Ahmed, Experimental and Theoretical NANOTECHNOLOGY 10 (2026) 343 https://doi.org/10.56053/10.s.343

*Exp. Theo. NANOTECHNOLOGY* 10 (2026) 535-549
[44] A. Khaleefah, M. RASHEED, Experimental and Theoretical NANOTECHNOLOGY 10 (2026) 289 https://doi.org/10.56053/10.s.289
[45] A. I. A. Ali, M. RASHEED, Experimental and Theoretical NANOTECHNOLOGY 10 (2026) 277 https://doi.org/10.56053/10.s.277
A. I. A. Ali, M. RASHEED, Experimental and Theoretical NANOTECHNOLOGY 10 (2026) 239 https://doi.org/10.56053/10.s.239